Transactions on Engineering Sciences vol 6, © 1994 WIT Press, www.witpress.com, ISSN 1743-3533

Delamination analysis for 2D- and 3D-models of a cross-ply laminated three-point bending specimen

H. Wang, S. Ding,* F.-G. Buchholz, R. Rikards#
Institute of Applied Mechanics, Paderborn University, Pohlweg 47-49, D-33098 Paderborn, Germany

ABSTRACT

An investigation was performed to study the delamination growth in two different cross-ply laminated three-point bending specimens. A two dimensional (2D) finite element (FE) analysis was firstly carried out to determine the strain energy release rates during the delamination of the beams. Contact elements were used to prevent the material interpenetration on the crack surfaces. To study three dimensional (3D) effects on the crack growth in the composite beams, 3D FE analysis was developed. The 3D results showed that the distribution of the energy release rates along the delamination front are not constant. At the free surface a coupling between mode II and mode III energy release rates was also observed, and it was further noticed that the dominating deformation mode is different for distinct laminate lay-ups even under a pure mode I loading condition. Comparison of the 2D and 3D FE analyses suggested that the critical delamination toughness obtained from 2D computations be conservative.

INTRODUCTION

Laminated composites have demonstrated their usefulness and potential increases in many structural applications. These materials must be designed to meet various engineering requirements and to withstand the service loads. Delamination is the major failure mode of laminated composites and is now widely investigated by static and/or low velocity impact loading tests. Delamination is initiated by two types of cracks: shear cracks in matrix and normal tension cracks perpendicular to fibres. These interlaminar cracks immediately propagate into ply interface and the associated stress concentration may then initiate delamination cracks. The initiation and growth of delamination is governed by the interlaminar fracture toughness of the material.

For most of the specimen geometries used in laminate testings it is possible to obtain analytical solutions using beam theory [1,2,3,4]. A general method for calculating the total energy release rates G_T from the local values of forces and

* Dept. of Matr. Sci and Eng., Oregon Grad. Inst., P.O. Box 91000, Portland, OR 97291-1000, USA.
# Dept. of Strength of Materials, Riga Tech. University, Kalku St. 1, LV 1047, Riga, LATVIA.

bending moments in a cracked laminates has been suggested by Williams [5]. These formulas [5] are the same as well known formulas for Double Cantilever Beam (DCB), End Notched Flexure (ENF) and other specimens developed previously by other methods. Formulas are simple only for the case of isotropic layers.

Fig. 1a shows a laminated cross ply beam with a central edge notch or edge crack in the bottom layer. In this case delamination crack with length **a** runs into the ply interface normal to the notch. This case of delamination growth due to bending in graphite/epoxy laminates was investigated by Sun [6]. A formula to calculate the total energy release rate was also given as

$$G_T^{REF}(a) = \frac{1}{2}\left[\left[\frac{A_{11}}{D}\right]_1 - \left[\frac{A_{11}}{D}\right]_2\right]\cdot\left[\frac{P^2}{4}\right]\cdot(a-L)^2 \qquad (1)$$

Here $D = A_{11} \cdot D_{11} - B_{11}^2$, where A_{11}, B_{11} and D_{11} are beam stiffnesses, and subscripts 1 and 2 denote values in section 1 and 2 respectively (see Fig. 1b).

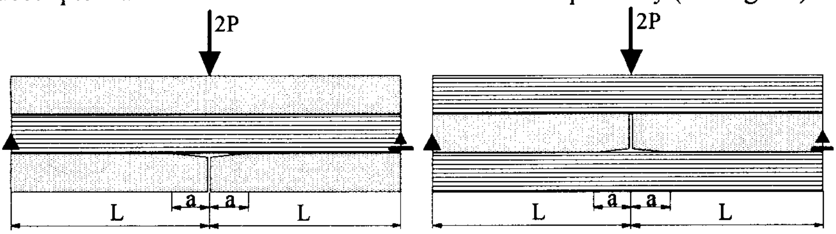

a) case 1 (90°/0°/90°) b) case 2 (0°/90°/0°)

Fig. 1: Geometry of 3-point bending specimen

The method discussed above gives total energy release rate $G_T = G_I + G_{II}$. In fact for this specimen there exists mixed mode fracture [6]. With this analysis it is impossible to separate energy release rate for opening G_I and the sliding or shear mode G_{II}. Mode partitioning is possible only using FE analysis [8].

By studying 3D effects on the energy release rate partitioning, Buchholz [11] analysed an isotropic crack and found that all mode I, II and III deformation presented at the crack tip irrespective of the loading condition. The mode-mixing effect became more apparent when the free surface was approached. Similar investigations on the composite beams were also conducted in this study to reveal the 3D influences on the laminate delamination toughness.

FINITE ELEMENT ANALYSIS

Two cases of three point bending specimens have been investigated. The first case is a 90/0/90 cross-ply laminated beam (see Fig. 1) with centre edge notch in the bottom layers. In this case delamination crack runs into the interface between layers parallel to the fibre direction. The delamination crack growth due to bending crack in graphite/epoxy laminate was also investigated elsewhere [6,7]. The second case is a 0/90/0 cross-ply laminated beam (see Fig. 1b) with centre notch in the middle layer. This specimen is for modelling initial shear crack in the matrix. Delamination crack growth induced by shear crack in matrix

is also on the 0/90 interface between layers. In this case there is crack surface interpenetration. To obtain exact mixed mode energy release rates contact problem on crack surface should be solved.
Strain energy release rates G_I and G_{II} for mixed mode delamination fracture are calculated by one calculation (1C) and global energy method (EN3) [8,9]. Finite element solution is obtained using program ABAQUS [10]. The mesh for 2D model is illustrated in Fig. 2.

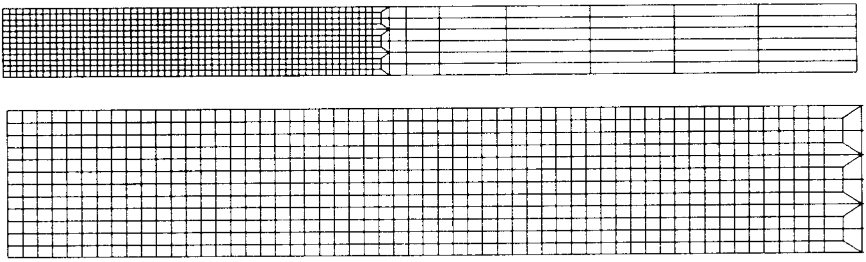

Fig. 2: Mesh for 2D-Model

The elastic material properties of graphite/epoxy used in the analysis are shown in Table 1. Where E, G and ν are Young's moduli, shear moduli and Poisson's ratio correspondingly. The subscript 1 denotes the fibre direction and subscripts 2 and 3 denote transverse directions. Half of the beam is analysed with a plane strain condition (see Fig. 1). The total load is P=2N/mm. The element edge length near the crack tip is Δa=0.2 mm.

TABLE 1 Material properties

E_{11}	=	119.9	GPa	($1.199*10^5$ N/mm^2)
E_{22}, E_{33}	=	9.86	GPa	($9.86*10^3$ N/mm^2)
G_{12}, G_{13}	=	5.24	GPa	($5.24*10^3$ N/mm^2)
G_{23}	=	3.52	GPa	($3.52*10^3$ N/mm^2)
ν_{12}, ν_{13}	=	0.3		
ν_{23}	=	0.4		

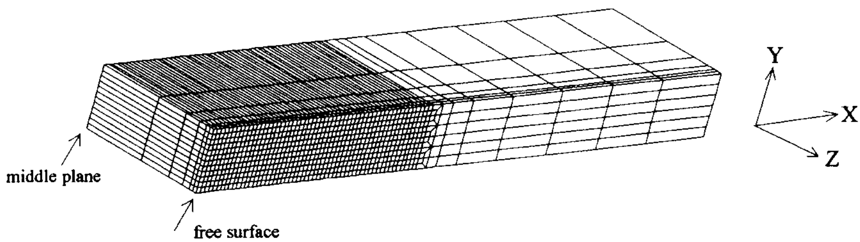

Fig. 3: Mesh for 3D model

A schematic of the 3D model is illustrated in Fig. 3. It has the same dimensions in the x-y plane and exactly the same material properties for case 1 and case 2 respectively as in the 2D situation. The third dimension is 10 mm in the z-direction. Considering the quarter symmetry in the x-z plane, the first quarter is selected to conduct the computation (Fig. 3). Eight-noded brick element is employed to discretise the object. With the confidence obtained from the 2D cases, all the energy release rates for 3D cases are evaluated via 1C method.

RESULTS AND DISCUSSION

For case 1 the displaced 2D mesh is shown in Fig. 4. It is evident that at the crack tip there exists normal tension crack (Mode I) and shear deformation (Mode II) simultaneously.

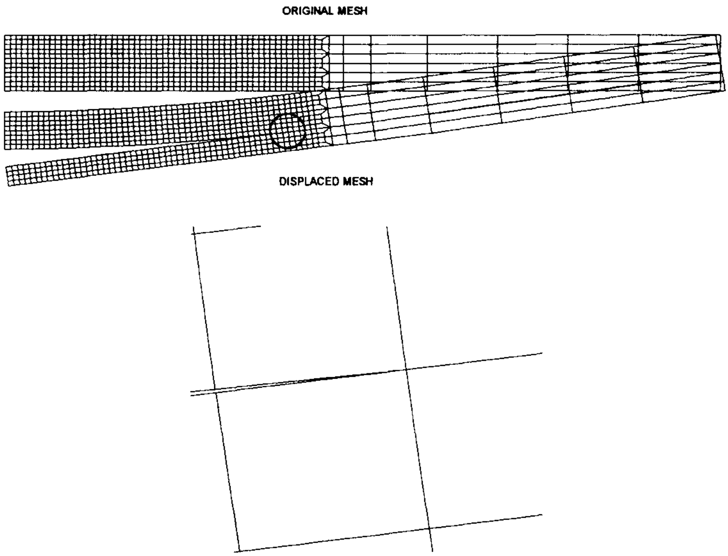

Fig. 4: Displaced mesh for 2D model (case 1)

Mixed mode energy release rates and total energy release rate (2D model), which are calculated with 1C and EN3 method, are presented in Fig. 5. For the first case the total energy release rate G_T agrees with the analytical solution from equation (1). A good agreement with 1C and EN3 method is also observed. In this case Mode I dominates. It should be also noted that the strain energy release rate for a fixed load decreases as the crack length increases. This indicates that delamination crack growth in this specimen is stable.

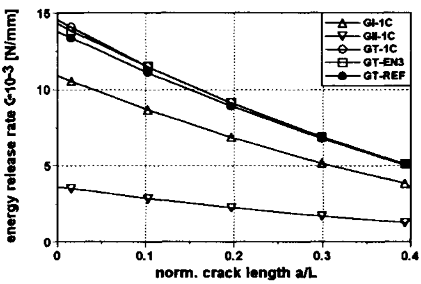

Fig. 5: Energy release rates for case 1

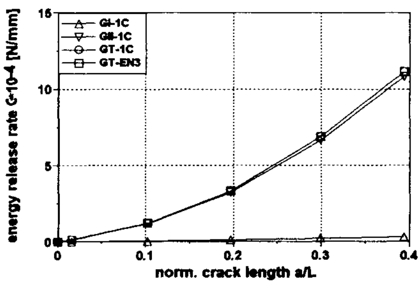

Fig. 6: Energy release rates for case 2

For case 2 there is interpenetrating (overlapping) of crack surfaces. Taking into account that opposite crack sides is in contact, this problem is solved as a contact problem using Coulomb's friction law on the crack surface. The displaced 2D mesh of this case is illustrated in Fig. 6. It shows that there is shear deformation (Mode II) at the crack tip.

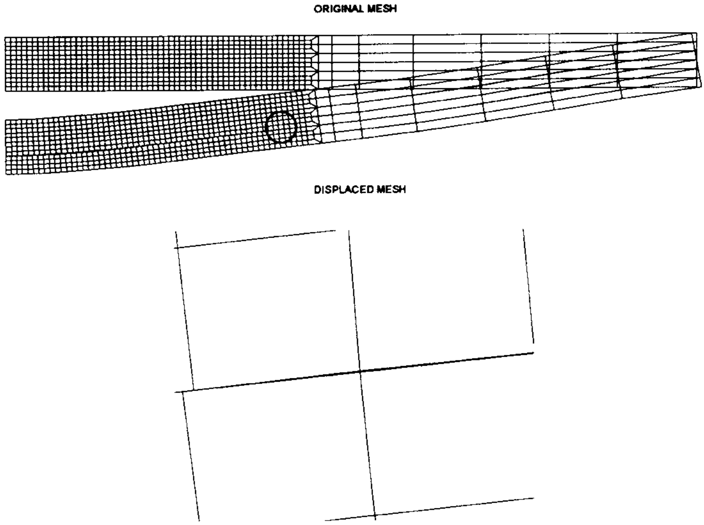

Fig. 7: Displaced mesh for 2d model (case 2)

Energy release rates for case 2 are presented in Fig. 6. As shown in Fig. 6, the results indicate that delamination crack growth in this specimen is unstable and Mode II predominates over Mode I.

The total energy release rates for case 1 and 2 are plotted in Fig. 8a and b respectively in a 3D sense. To have a detailed examination on the relative relations among G_I, G_{II}, G_{III} and G_T, a cross-sectional cut from Fig. 8a is shown in Fig. 9a, where, as expected, mode III deformation is observed when the free surface is approached. Similar efforts have been done to case 2 and the plot is illustrated in Fig. 9b. Global deformations of the specimens in the 3D situation for case 1 and 2 are similar to those of the 2D (Figs. 4 and 7) However, the local deformations on the crack tips are different from the 2D's and are depicted in Fig. 10.

As stated in the introduction section, it was noted that in the isotropic material cases there always exists a mixed mode deformation in the vicinity of crack front meeting the free surface [11] irrespective of the loading mode. By examining Fig. 9, it is evident that this observation is also true for composite materials since G_I and G_{II} always co-exist and G_{III} arises when the free surface comes close to the point of interest. In addition, in Fig. 10, the mixed mode deformation can also be observed, and it is further noticed that the middle layer in case 1 shrinks and that in case 2 expands in the z-direction due to effect of individual laminate lay-ups and the central notch position.

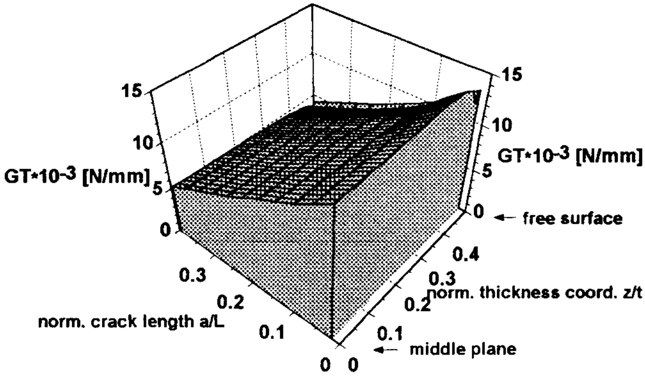

a) case 1

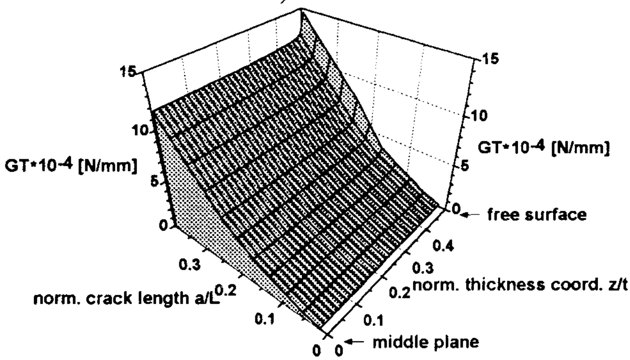

b) case 2

Fig. 8: Distribution of the total energy release rate

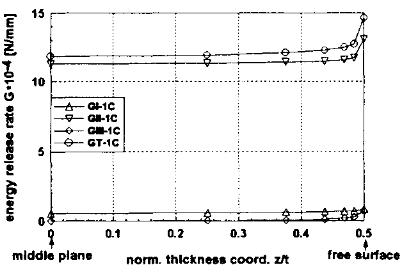

a) a/L = 0.01575, case 1

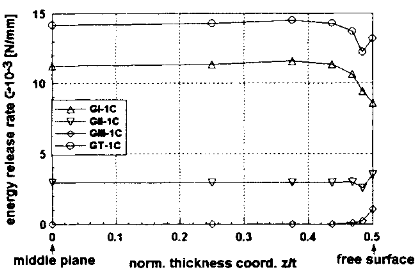

b) a/L = 0.3937, case 2

Fig. 9: Energy release rate partitioning

The deformation modes along the crack front are well partitioned in Fig. 9. It is noted that individual components of the energy release rate almost keep constant when z/t is smaller than 0.4. Beyond this point, z/t > 0.4, the partition ratios begin to change noticeably. This may be caused by the emergence of G_{III}. However, the effect of G_{III} getting bigger as z/t increases is different for case 1 and 2. For case 1, as z/t increases G_I and G_T decrease, and G_{II} increases except a small shallow curve (Fig. 9). In case 2, all the components increment when increasing z/t. The G_T distribution along the crack front for case 1 and case 2 will result in different shapes of crack front line, that is, from the view point of the total energy release rate distribution, it may be predicted that the crack front line for case 1 will be parabola-like with its most front point in the middle plane; while in case 2, the most front point of the crack tip line will be at the two free surfaces.

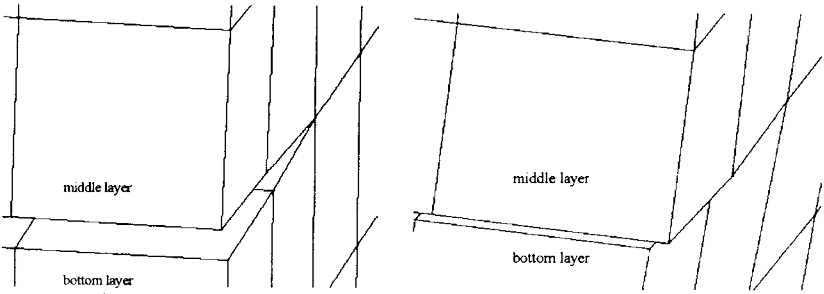

a) case 1 b) case 2

Fig. 10 Local deformation of the crack tip near the free surface

Comparing the results from the 2D (Figs. 5 and 6) and 3D (Figs. 8 and 9) it is noted that the observations in 2D, that in case 1 node I dominates and the crack is stable, while in case 2 the dominating deformation is mode II and the failure will be catastrophic whenever it starts, is also true for the 3D situation. However, the values of the individual energy release rate components are different, that is, for the same crack length, the 3D solution is always greater than the 2D's. This observation may imply that the critical delamination toughness obtained from 2D analysis is conservative in practice.

CONCLUSION

Analyses of 2D and 3D FEM solutions in cross ply laminates for delamination cracks initiated by bending and shear cracks were carried out. Energy release rates using modified virtual crack closure integral methods were obtained. Comparison of total energy release rates obtained by local energy methods with analytical solution and global energy method have been conducted. Good agreement of the results obtained by various methods has been observed. The deformation at the crack tip will be mixed in nature irrespective of the loading mode, but the dominating mode of deformation and the front line shape of the delamination crack will depend on the laminate lay-ups and the central notch position. FEM solutions obtained above for these two cross ply laminated three point bending beam specimens can be used to estimate in experiment the critical energy release rates in delamination cracks although the 2D solutions may be a little conservative.

ACKNOWLEDGEMENTS

This work was supported by the Commission of European Communities through Contract ERB-CIPA-CT-92-2071, proposal No. 3576, in the framework of Community's Action for Co-operation in Sciences and Technology with Central and Eastern European Countries. Other supports also came from the Institute of Applied Mechanics, Paderborn University, Germany, Department of Strength of Materials, Riga Technical University, Latvia, and the Department of Materials Science and Engineering, Oregon Graduate Institute of Science & Technology, USA.

REFERENCE

1. Sjöblom, P.O., Hartness, J.T., "On Low-Velocity Impact Testing of Composite Materials" *J. Composite Materials*, Vol.22, pp.30-52, 1988
2. Wu, H.-Y.T., Springer, G.S., "Measurements of Matrix Cracking and Delamination Caused by Impact on Composite Plates" *J. Composite Materials*, Vol.22, pp. 518-532, 1988
3. Maikuma, H., Gillespie, J.W., Jr., Wilkins, D.J., "Mode II Interlaminar Fracture of the Center Notch Flexural Specimen under Impact Loading" *J. Composite Materials*, Vol.24, pp.124-149, 1990
4. Doxsee, L.E., Rubbrecht, P., Li, L., Verpoest, I., Scholle, M., "Delamination Growth in Composite Plates Subjected to Transverse Loads" *J. Composite Material*, Vol.27, No.8, pp.764-781, 1993
5. Williams, J.G., "On the Calculation of Energy Release Rates for Crack Laminates" *Int. J. of Fracture*, Vol.36, pp.101-119, 1988
6. Sun, C.T., Manoharan, M.G., Growth of Delamination Cracks Due to Bending in a [90/0/90] Laminate" *Composite Science and Technology*, Vol.34, pp.365-377, 1989
7. Jih, C.j., Sun, C.T., Prediction of Delamination in Composite Laminates Subjected to Low Velocity Impact. *J. Composite Materials*, Vol.27, No.7 pp. 684-701, 1993
8. Rybicki, E.F., Kanninen, M.F., "A Finite Element Calculation of Stress Intensity Factors by Modified Crack Closure Integral" *Eng. Fracture Mechanics*, Vol.9 pp. 931-938, 1977
9. Buchholz, F.-G., "Improved Formulae for the Finite Element Calculation of the Strain Energy Release Rate by Modified Crack Closure Integral Method" in Accuracy, Reliability and Training in FEM Technology (Ed. Robinson, J.), pp. 650-659, *Proc. of the 4th World Congr. and Exib. on Finite Element Methods*, Interlaken, Switzerland, 1984
10. Hibbitt, Karlsson and Sorensen Inc., *ABAQUS User's Manual*, Version 5.3, Providence Rhode Island, 1993
11. Buchholz, F.-G., "Mixed-Mode und Mehrachsigkeitseinflüsse bei der FE-Analyse von CTS-Proben endlicher Dicke" In Deutscher Verband für Materialforschung und -prüfung (DVM), pp.371-381, *Proc. der 25 Vortragsveranstaltung des DVM-Arbeitskreises Bruchvorgänge*, Karlsruhe, Deutschland, 1993.